Highly conductive group VI transition metal dichalcogenide films by solution-processed deposition

Wooseok Ki, Xiaoying Huang, and Jing Li[a)]
Department of Chemistry and Chemical Biology, Rutgers University, Piscataway, New Jersey 08854

David L. Young and Yong Zhang
National Renewable Energy Laboratory, Golden, Colorado 80401

A new soluble synthetic route was developed to fabricate thin films of layered structure transition metal dichalcogendies, MoS_2 and WS_2. High-quality thin films of the dichalcogenides were prepared using new soluble precursors, $(CH_3NH_3)_2MS_4$ (M = Mo, W). The precursors were dissolved in organic solvents and spun onto substrates via both single- and multistep spin coating procedures. The thin films were formed by the thermal decomposition of the coatings under inert atmosphere. Structural, electrical, optical absorption, thermal, and transport properties of the thin films were characterized. Surface morphology of the films was analyzed by atomic force microscopy and scanning electron microscopy. Highly conductive and textured *n*-type MoS_2 films were obtained. The measured room temperature conductivity ~50 Ω^{-1} cm^{-1} is substantially higher than the previously reported values. The *n*-type WS_2 films were prepared for the first time using solution-processed deposition. WS_2 displays a conductivity of ~6.7 Ω^{-1} cm^{-1} at room temperature.

I. INTRODUCTION

Solution-based deposition techniques, such as printing[1] and spin casting,[2,3] have been well developed to fabricate thin-film transistors (TFTs). Spin-coating techniques have apparent advantages for fabrication of low-cost, flexible, and large-area devices and have been widely used to obtain uniform and continuous films. Most metal chalcogenide semiconductors exhibit poor solubility in common solvents, which limits the utility of solution-processed deposition. Recently, Mitzi et al. have demonstrated that by use of soluble precursors such as hydrazinium salts, binary metal chalcogenide TFTs (e.g., SnS_2 and In_2Se_3) can be processed via spin-coating techniques.[2,4]

Transition metal dichalcogenides (TMDCs) are a group of inorganic materials with both fundamental and technological importance. They have been used in numerous applications, such as lubricants, catalysis, and solar cells.[5–7] It has been demonstrated that micro- and/or nano-structures of TMDCs can be obtained from thermal decomposition of ammonium thiosalts at various temperatures.[8–10] Synthetic routes used to produce TMDC thin films include sulphurization,[11] electrodepo-

sition,[12] sputtering/annealing,[13,14] chemical bath depositions,[15] and thermal decomposition.[16] Most thin film fabrication methods mentioned above require high vacuum or high temperatures. Very little has been reported on solution-based deposition of Group-VI metal dichalcogenides. For example, spin-coated MoS_x thin films have been reported only for tribological applications,[17] and to the best of our knowledge, no study has been reported on solution-processed tungsten dichalcogenide thin films. In this work, we report highly conductive *n*-type MoS_2 and WS_2 thin films obtained by a very simple solution process employing spin-casting techniques.

II. EXPERIMETNAL

A. Preparation of precursors

To prepare the soluble precursors, 1.5 mmol $(NH_4)_2MoS_4$ (99.99%, Alfa Aesar, Ward Hill, MA) was dissolved in 1.2 ml methylamine (40 wt%, aqueous solution). The dark red clear solution was obtained with constant stirring in an argon atmosphere at room temperature. This solution was then dried in a vacuum oven overnight at room temperature. Dark red crystals of $(CH_3NH_3)_2MoS_4$ were collected. Crystal data are given below: $C_2H_{12}MoN_2S_4$, *Fw* = 288.32, orthorhombic *Pnma*, a = 9.636(2)Å, b = 6.9820(10)Å, c = 15.763(3)Å, V = 1060.5(3)Å^3, Z = 4. $(CH_3NH_3)_2WS_4$ precursors were also prepared by dissolving 1.4 mmol $(NH_4)_2WS_4$ (99.99%, Aldrich, Milwaukee, WI) in 1 ml

methylamine. A yellowish orange clear solution was obtained with constant stirring in an argon atmosphere at room temperature. After the solution was dried in a vacuum oven overnight at room temperature, yellow crystals of $(CH_3NH_3)_2WS_4$ were collected. The crystal data are given below: $C_2H_{12}N_2S_4W$, $Fw = 376.23$, Orthorhombic $Pnma$, $a = 9.692(2)$Å, $b = 7.0400(10)$Å, $c = 15.745(3)$Å, $V = 1074.3(3)$Å^3, $Z = 4$.

B. Preparation of MoS₂ thin films

To prepare MoS_2 thin films, the $(CH_3NH_3)_2MoS_4$ crystals (0.1687 g) were dissolved completely in 1 ml ethylene glycol (99.9%, Fisher, Fairlawn, NJ) at room temperature in an argon atmosphere. Thermally grown oxidized silicon substrates ($d_{SiO_2} = 4000$ Å) were cleaned by the piranha method.[4] The substrates were dipped in a solution mixture containing a 4:1 volume ratio of 95% H_2SO_4 and 35%H_2O_2 and heated to 90 °C for 15 min. The cleaned silicon substrates were then rinsed by distilled water and cleaned again in a solution of 30%NH_4OH, 35%H_2O_2, and H_2O in 1:1:5 (vol%) ratio at 70 °C for 10 min and rinsed with distilled water. A deep red solution of $(CH_3NH_3)_2MoS_4$ was spun onto SiO_2/Si substrate at 3500 rpm for 60 s and dried at 70 °C for a few seconds in air on a hot plate. This spin-casting sequence was repeated 5 times to improve continuity and uniformity of the surface. The MoS_2 thin films formed after a two-step calcination process (200 °C for 1 h and 600 °C for 2 h under N_2).

C. Preparation of the WS₂ thin films

To prepare WS_2 thin films, the $(CH_3NH_3)_2WS_4$ crystals (0.2520 g) were dissolved in 0.8 ml of hydrazine (98.5%, Alfa Aesar), deposited by a spin coater at 3500 rpm for 1 min onto SiO_2/Si and dried at 60 °C for a few minutes in air on a hot plate. The WS_2 thin films were formed after the same two-step calcination process described above. The crystallinity of WS_2 film was much improved, when hydrazine was used as a solvent after calcination. On the other hand, the WS_2 films show very broad powder x-ray diffraction (PXRD) peaks when synthesized in an ethylene glycol solvent.

D. Characterization of the thin films

PXRD was performed on all films using a Rigaku (Tokyo, Japan) D/M-2200T automated diffraction system (Ultima+). Single-crystal x-ray diffraction was carried out to determine the crystal structures of the both precursors with an Enraf-Nonius (Bohemia, NY) CAD4 diffractometer with graphite monochromated Mo K_α radiation at 293 K. Optical diffuse reflectance was measured by a Shimadzu (Kyoto, Japan) UV-3101PC double beam, double monochromated spectrophotometer at room temperature in the range of 250–2000 nm. Esti-

mated band gaps were obtained by converting the data to the Kubelka–Munk function.[18] Thermogravimetric (TG) analysis of both precursors was performed on a TA Instruments (New Castle, DE) TG Q50 analyzer with a ramp rate of 5 °C/min from room temperature to 600 °C under N_2 atmosphere. Surface morphology of thin films was investigated on an atomic force microscope (AFM) (Q-scope 350, Quesant, Santa Cruz, CA) in the tapping mode. Film thickness was measured by scanning electron microscope (SEM; 6320F Field Emission Electron Microscope, JEOL, Tokyo, Japan). The temperature-dependent electrical resistivity of the films was obtained by the direct current (dc) four-point probe method using silver paint electrodes on the film surface in the temperature range of 25–300 K. Room-temperature conductivity and Hall effect measurements were made on a BioRad (Milpitas, CA) HL5500IU Hall system. Ohmic contacts were made to the films by pressing indium metal onto the surface of the films.

III. RESULTS AND DISCUSSION

A. MoS₂ thin films

The crystal structure of the $(CH_3NH_3)_2MoS_4$ precursor is shown in Fig. 1. Compared with the starting material $(NH_4)_2MoS_4$, $(CH_3NH_3)_2MoS_4$ exhibits significantly enhanced solubility (up to 70% at room temperature, 1 atm) in the solvents used for film deposition and much improved morphology and crystallinity of films. Thermal decomposition of this precursor was performed from room temperature to ~600 °C by thermogravimetric analysis (TGA) under N_2 atmosphere. As seen in Fig. 2, the final product was identified as MoS_2 after a 44.4% weight loss of organic component, which is in excellent agreement with the calculated value of 44.5%. Dissolved samples of precursors were drop cast and annealed on clean glasses and used for characterization of the structure and optical properties by PXRD and ultraviolet-visible (UV-VIS) spectroscopy. Figure 3(a) shows the PXRD patterns of the thin film samples calcinated at (i) 450 and (ii) 600 °C, respectively. They are compared with the PXRD of the 2H–MoS_2 taken from the ICDD database (ICDD 37-1492).[19] Clearly, films calcined at higher temperature (i.e., 600 °C) show higher crystallinity and more preferred orientation corresponding to the (00l) plane. The shift of the first peak to a lower angle (~0.2 Å) was also observed by Pütz et al.[17] The band gap was estimated to be 1.5–1.6 eV [Fig. 3(b)], slightly smaller than previously reported data for 2H–MoS_2.[20] Film morphology is highly dependent on the choice of solvents, as well as the spin coating procedure. Depending on the solvent used and spin coating sequence, dramatically different grain morphology and surface coverage may result. As shown in Fig. 4(a), when ethylene glycol was chosen as the solvent, spherical grains with an
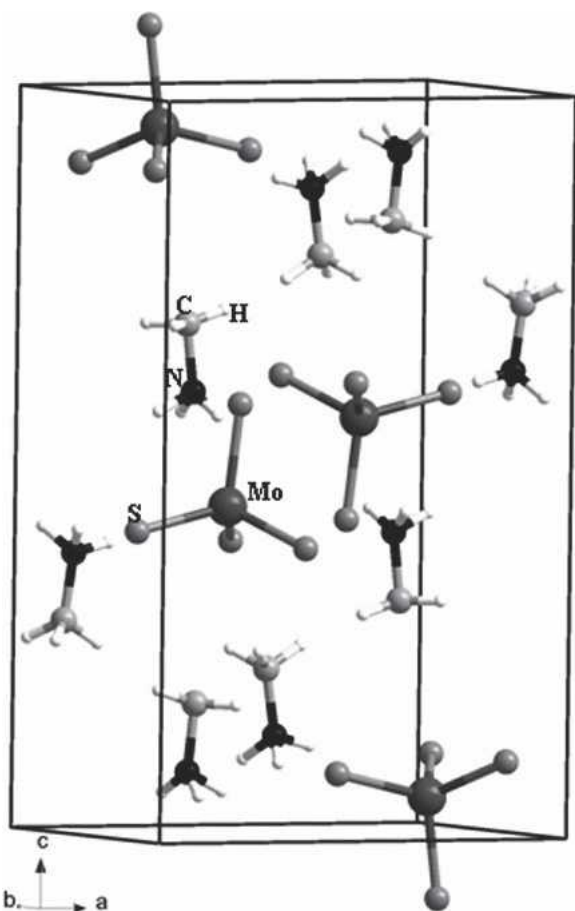
FIG. 1. View of the molecular crystal structure of $(CH_3NH_3)_2MoS_4$.

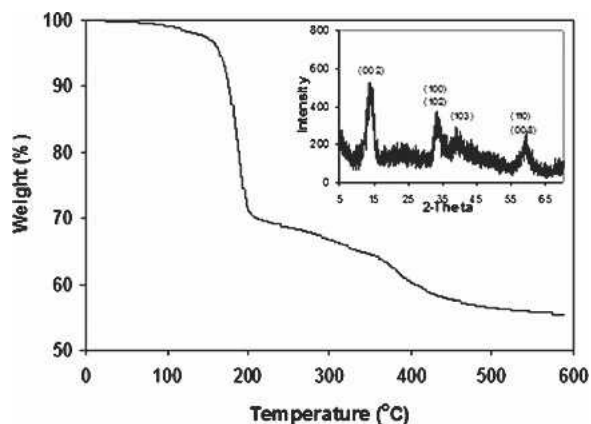FIG. 2. Thermogravimetric analysis of $(CH_3NH_3)_2MoS_4$ (ramp rate: 5 °C/min). (inset) PXRD pattern after thermal decomposition of the precursor at ~600 °C. The final product is 2H–MoS$_2$ from the ICDD database.

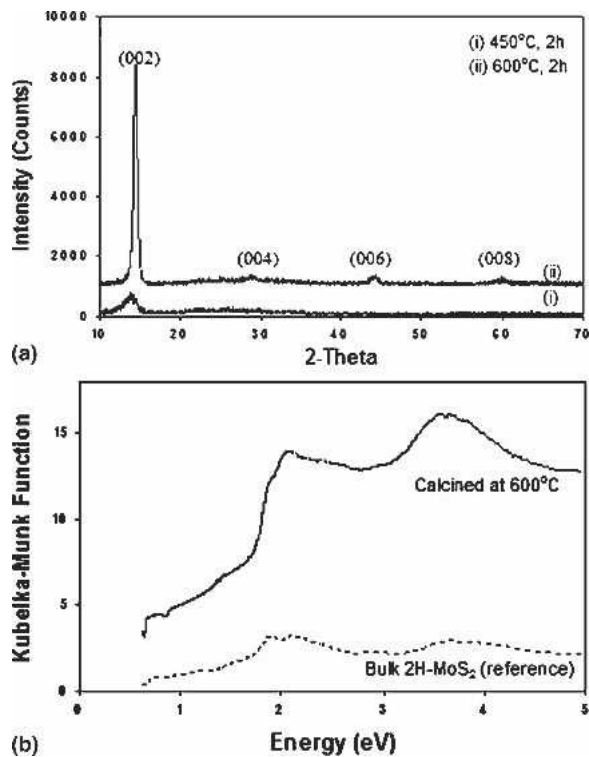

FIG. 3. (a) PXRD patterns of the MoS$_2$ films deposited onto glass slides: (i) 450 °C and (ii) 600 °C. (b) Optical absorption spectra of the 2H–MoS$_2$ taken between 250 and 2000 nm; (solid line) film sample calcined at 600 °C, (dashed line) powder sample purchased from Aldrich.

average size of ~300 nm were formed by applying single-step spin coating (with a standard deviation of ~100 nm), while multistep process yielded a more continuous and well-connected film with significantly larger grain sizes [average size ~1.8 μm, Fig. 4(b)]. Clearly, the thin plate-shaped crystals have a preferential orientation of (00l), as

seen in Fig. 4(b). However, when hydrazine, a strong reducing agent, was used as the solvent, ellipsoid shaped grains (size ~1μm) were created in the MoS$_2$ films by multistep spin coating. In addition, films were discontinuous and inhomogeneous. As a result, the resistance of MoS$_2$ film was much higher with hydrazine (~1.6 MΩ) than it was with ethylene glycol (~1 KΩ). Ethylene glycol has a high viscosity (~16 cp at room temperature) and good wetting ability. Moreover, it is favored over highly toxic hydrazine, because ethylene glycol is environmentally safe.

The resistivity of the films was calculated from sheet resistance by the four-point probe method with the film thickness of ~70 nm, as shown in Fig. 5, and was found to be ~0.02 Ω cm at room temperature. This value is at least an order of magnitude smaller than the previously reported values.[15,21–23] As shown in Fig. 6, the resistivity slightly increases with an increase in temperature, indicating metal-like behavior. The metallic nature and low resistivity of these films may be attributed to high electron concentration obtained by Hall measurements (see Table I), which is higher than that typically found in single crystals (10^{16} to 10^{17} cm^{-3}).[24] In addition, as seen in the surface topology of the films shown in Fig. 4, single-step spin coating resulted in small grain size and
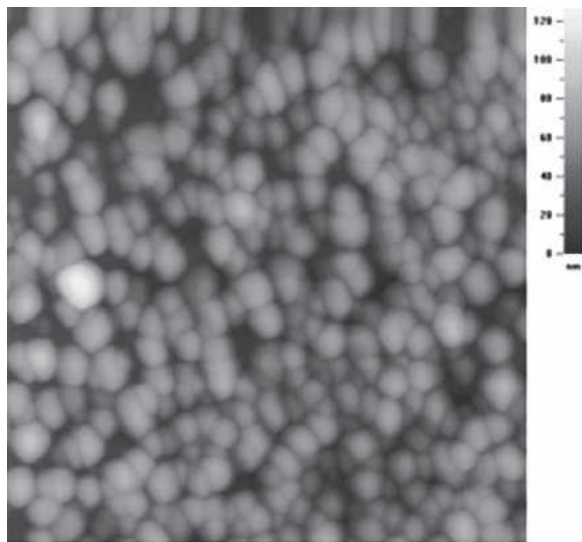
(a)
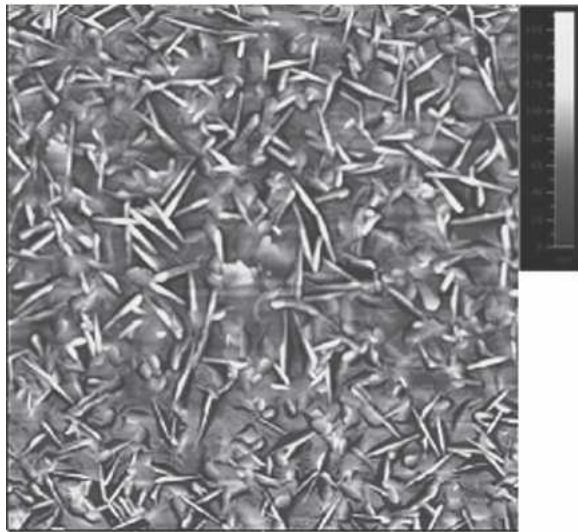
(b)

FIG. 4. AFM images of the MoS$_2$ thin films taken with tapping mode: (a) Single-step spin-cast sample with a 5 μm × 5 μm scan; average film thickness is ~45 nm by AFM. (b) Multistep spin-cast sample with a 20 μm × 20 μm scan; average thickness is ~70 nm by SEM (see Fig. 5). In both cases, ethylene glycol was used as solvent.

high grain boundary area and, consequently, higher resistivity (~10 Ω cm). On the other hand, the films processed by multistep spin coating sequence show fewer grain boundaries and are highly continuous. As a consequence, their resistivity is significantly lowered by two orders of magnitude. Another possibility to explain high conductivity is that even though the film is primarily the crystalline MoS$_2$ phase, there maybe a small amount of impurity in the MoS$_2$ film (i.e., MoS$_{2\pm x}$) from thermal decompositions that account for the increased conductivity.[25] Table I shows transport data on the films from the Hall effect measurements. The uncertainty in the values is about 10%. The Hall measurements indicate electron
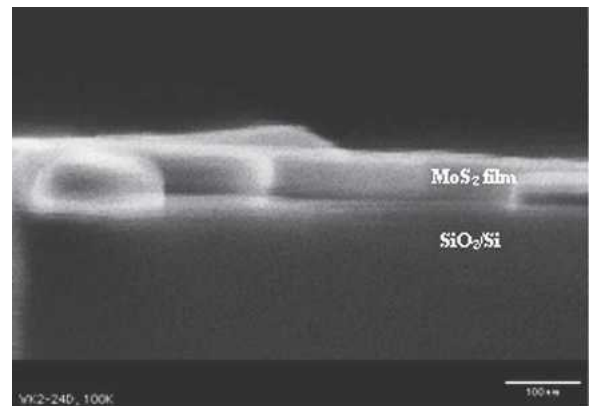

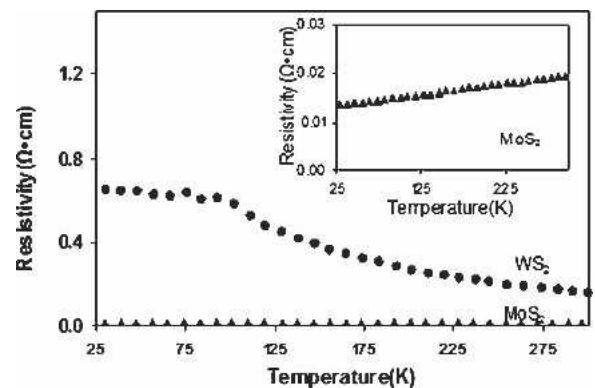FIG. 5. Cross-sectional SEM image of the MoS$_2$ thin film by mutistep spin coating (scale bar: 100 nm).

FIG. 6. Resistivity of MoS$_2$ and WS$_2$ thin films as a function of temperature by four-point probe methods. (inset) Resistivity of MoS$_2$ plotted at an enlarged scale.

TABLE I. Transport data measured on MoS$_2$ and WS$_2$ thin films.

	Mobility (cm^2/Vs)	Carrier concentration (cm^{-3})
WS$_2$	<1	n-type
MoS$_2$	2	n-type 2×10^{20}

conduction in the MoS$_2$. While the MoS$_2$ film exhibits a higher conductivity, the carrier mobility is relatively low. Low mobility of the films could be explained by impurity scattering.[26] As shown in Fig. 3(a), lattice distortion occurred at every peak position. Based on the lattice expansion equation $\epsilon = \Delta d/d_o$ (d_o is the d-spacing of the original lattice; Δd is the change in the d-spacing; ϵ is the lattice expansion)[27] the lattice expansion of the (002) plane of the MoS$_2$ was calculated to be 1.5% at 600 °C and 3.2% at 450 °C. For the MoS$_2$ films, this lattice distortion may arise from carbon impurities, as previously reported.[17]

B. WS$_2$ thin films

The crystal structure of (CH$_3$NH$_3$)$_2$WS$_4$ is isostructual to that of (CH$_3$NH$_3$)$_2$MoS$_4$ (Fig. 1). Its thermal decomposition properties were also analyzed by TGA under
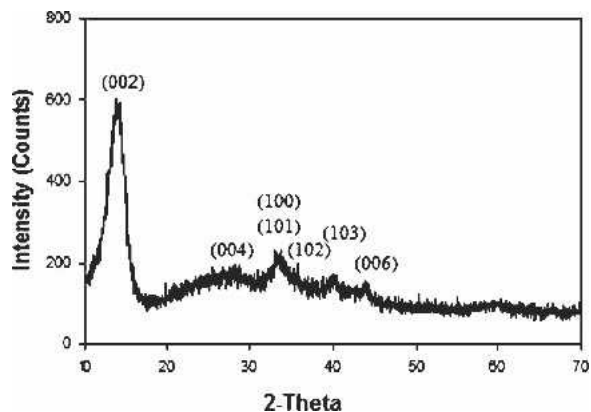
FIG. 7. PXRD pattern of a WS$_2$ thin film spun onto a glass (after annealing at 600 °C under H$_2$/Ar).

FIG. 9. Cross-sectional SEM image of the WS$_2$ thin film by single-step spin coating (scale bar: 100 nm).

inert nitrogen atmosphere. The final product was a mixture of WO$_3$ and WS$_2$ because tungsten oxide is more stable than molybdenum oxide based on their free anthalpy data.[27] To avoid WO$_3$, the WS$_2$ films were processed under a flow of hydrogen/argon at 600 °C. The PXRD pattern of a typical WS$_2$ thin film is shown in Fig. 7 in comparison with that of 2H–WS$_2$ bulk (ICDD 08-0237).[19] In general, the peaks are broad, possibly due to relatively poor crystallinity. Average particle size of the films was estimated to be ~100 nm. It has been reported that highly crystalline WS$_2$ may be achieved by thermal decomposition of ammonium tetrathiotungstate at very high temperatures (over 1000 °C).[29] The first diffraction peak also shifted slightly to a lower angle, as in the case of MoS$_2$. Optical absorption experiments revealed a very weak absorption. The optical band gap of WS$_2$ film was consistent with the reported value of 1.3 eV.[20] The AFM image of a WS$_2$ film is shown in Fig. 8. Uniform and continuous films were obtained by a single-
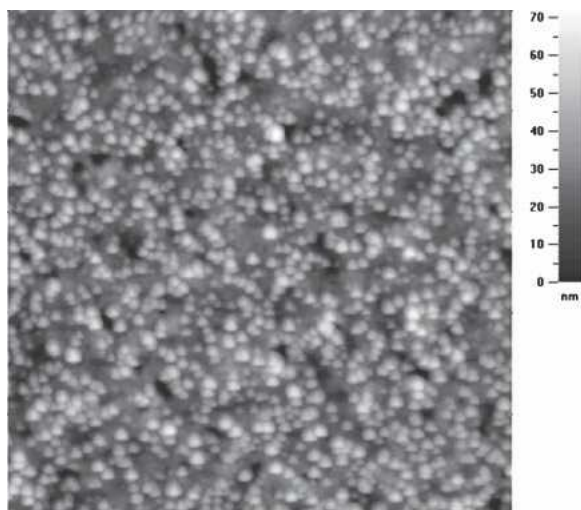
step spin coating procedure because multistep spin coating did not lead to uniform surface of WS$_2$ films as in the case of the MoS$_2$. Thus, surface morphology is again strongly case dependent. The average thickness of the films is ~50 nm, as shown in Fig. 9. Temperature dependence of the electrical resistivity was measured and plotted in Fig. 6. The WS$_2$ films show a typical semiconductor behavior. The resistivity of the film was found to be ~0.15 Ω cm at room temperature, which is lower than that of WS$_2$ films synthesized by other techniques.[11,14,30] Because of low carrier mobility, the Hall measurement on WS$_2$ films has some uncertainty, but the thermal probe does indicate the films are *n*-type.

IV. CONCLUSION

In summary, we have developed a simple, efficient, and low-cost solution-processed deposition route to fabricate MoS$_2$ and WS$_2$ thin films by using soluble precursors via the spin-coating technique. Surface morphology, such as grain size and continuity of the films, was directly influenced by the choice of organic solvents used to dissolve the precursors, as well as spin-coating sequences. Morphological changes affected the conductivity of the films. Highly conductive and textured *n*-type MoS$_2$ thin films were achieved by multi-step spin casting using ethylene glycol as the solvent. The *n*-type WS$_2$ thin films were fabricated using soluble precursors via single-step spin coating.

ACKNOWLEDGMENTS

FIG. 8. AFM image of WS$_2$ thin film by single-step spin casting (size of the image: 5 μm × 5 μm). Average size of the grain is ~100 nm, and thickness of the films is ~50 nm by SEM.
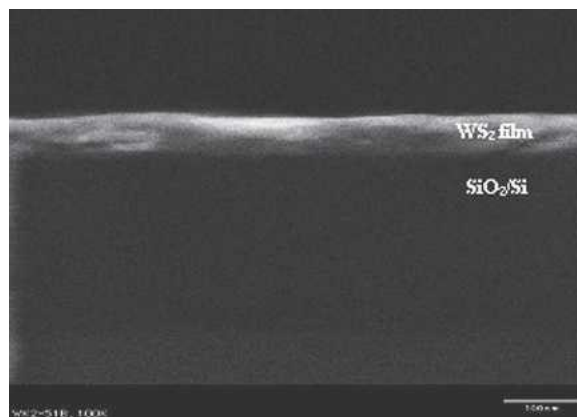
REFERENCES

1. B.A. Ridley, B. Nivi, and J.M. Jacobson: All-inorganic field effect transistors fabricated by printing. *Science* **286,** 746 (1999).

2. D.B. Mitzi, M. Copel, and S.J. Chey: Low-voltage transistor employing a high-mobility spin-coated chalcogenide semiconductor. *Adv. Mater.* **17,** 1285 (2005).

3. C.R. Kagan, D.B. Mitzi, and C.D. Dimitrakopoulos: Organic-inorganic hybrid materials as semiconducting channels in thin-film field-effect transistors. *Science* **286,** 945 (1999).

4. D.B. Mitzi, L.L. Kosbar, C.E. Murray, M. Copel, and A. Afzall: High-mobility ultrathin semiconducting films prepared by spin coating. *Nature* **428,** 299 (2004).

5. L. Rapoport, Y. Bilik, Y. Feldman, M. Homyonfer, S.R. Cohen, and R. Tenne: Hollow nanoparticles of WS_2 as potential solid-state lubricants. *Nature* **387,** 791 (1997).

6. B. Hinnemann, P.G. Moses, J. Bonde, K.P. Jørgensen, J.H. Nielsen, S. Horch, I. Chorkendorff, and J.K. Nørskov: Biomimetic hydrogen evolution: MoS_2 nanoparticles as catalyst for hydrogen evolution. *J. Am. Chem. Soc.* **127,** 5308 (2005).

7. R.A. Simon, A.J. Ricco, J. Harrison, and M.S. Wrighton: Improvement of the photoelectrochemical oxidation of halides by platinization of metal dichalcogenide photoanodes. *J. Phys. Chem.* **87,** 4446 (1983).

8. J. Chen, S.L. Li, F. Gao, and Z.L. Tao: Synthesis and characterization of WS_2 nanotubes. *Chem. Mater.* **15,** 1012 (2003).

9. P. Afanasiev and I. Bezverkhy: Synthesis of MoS_x ($5 > x > 6$) amorphous sulfides and their use for preparation of MoS_2 monodispersed microspheres. *Chem. Mater.* **14,** 2826 (2002).

10. C.M. Zelenski and P.K. Dorhout: Template synthesis of near-monodisperse microscale nanofibers and nanotubules of MoS_2. *J. Am. Chem. Soc.* **120,** 734 (1998).

11. A. Jäger-Waldau, M.Ch. Lux-Steiner, G. Jäger-Waldau, and E. Bucher: WS_2 thin films prepared by sulphurization. *Appl. Surf. Sci.* **71,** 731 (1993).

12. J. Jebarj Devadasan, C. Sanjeeviraja, and M. Jayachandran: Electrodeposition of p-WS_2 thin film and characterization. *J. Cryst. Growth* **226,** 67 (2001).

13. C. Ballif, M. Regula, F. Lévy, F. Burmeister, C. Schäfle, T. Matthes, P. Leiderer, P. Niedermann, W. Gutmannsbauer, and R. Bucher: Submicron contacts for electrical characterization of semiconducting WS_2 thin films. *J. Vac. Sci. Technol., A* **16,** 1239 (1998).

14. S.J. Li, J.C. Bernède, J. Pouzet, and M. Jamali: WS_2 thin films prepared by solid state reaction (induced by annealing) between the constituents in thin film form. *J. Phys. Condens. Matter* **8,** 2291 (1996).

15. K.C. Mandal and A. Mondal: Chemically deposited semiconducting molybdenum sulfide thin films. *J. Solid State Chem.* **85,** 176 (1990).

16. D. Tonti, F. Varsano, F. Decker, C. Ballif, M. Regula, and M. Remškar: Preparation and photoelectrochemistry of semiconducting WS_2 thin films. *J. Phys. Chem. B* **101,** 2485 (1997).

17. J. Pütz and M.A. Aegerter: Spin deposition of MoS_x thin films. *Thin Solid Films* **351,** 119 (1999).

18. W.M. Wendlandt and H.G. Hecht, *Reflectance Spectroscopy* (Wiley Interscience, New York, 1966).

19. ICDD Card Nos. 37-1492 and 08-0237. International Center for Diffraction Data: Newton Square, PA, 1996.

20. E. Bucher and A. Aruchamy, *Photoelectrochemistry and Photovoltaics of Layered Semiconductors* (Kluwer Academic Publishers, Dordrecht, NL, 1992), p. 36.

21. J.C. Bernède, J. Pouzet, E. Gourmelon, and H. Hadouda: Recent studies on photoconductive thin films of binary compounds. *Synth. Met.* **99,** 45 (1999).

22. J. Cheon, J.E. Gozum, and G.S. Girolami: Chemical vapor deposition of MoS_2 and TiS_2 films from the metal-organic precursors Mo(S-t-Bu)$_4$ and Ti(S-t-Bu)$_4$. *Chem. Mater.* **9,** 1847 (1997).

23. N. Barreau and J.C. Bernède: MoS_2 textured films grown on glass substrates through sodium sulfide based compounds. *J. Phys. D Appl. Phys.* **35,** 1197 (2002).

24. J.A. Wilson and A.D. Yoffe: The transition metal dichalcogenides discussion and interpretation of the observed optical, electrical and structural properties. *Adv. Phys.* **18,** 193 (1969).

25. G. Alonso, V. Petranovskii, M. Del Valle, J. Cruz-Reyes, A. Licea-Claverie, and S. Fuentes: Preparation of WS_2 catalysts by in situ decomposition of tetraalkylammonium thiotungstates. *Appl. Catal. G E N* **197,** 87 (2000).

26. S.M. Sze: *Semiconductor Devices: Physics and Technology*, 2nd ed. (John Wiley & Sons, New York, 1985).

27. D. Mergel and Z. Qiao: Correlation of lattice distortion with optical and electrical properties of In_2O_3:Sn films. *J. Appl. Phys.* **95,** 5608 (2004).

28. J. Ouerfelli, J.C. Bernède, A. Khelil, and J. Pouzet: Photoconductive WS_2 thin films obtained from multilayer Ni/W/S . . . W/S structure. *Appl. Surf. Sci.* **120,** 1 (1997).

29. R.I. Walton and S.J. Hibble: A combined in situ x-ray absorption spectroscopy and x-ray diffraction study of the thermal decomposition of ammonium tetrathiotungstate. *J. Mater. Chem.* **9,** 1347 (1999).

30. K. Ellmer, C. Stock, K. Diesner, and I. Sieber: Deposition of c⊥-oriented tungsten disulfide (WS_2) films by reactive DC magnetron sputtering from a W-target in Ar/H_2S. *J. Cryst. Growth* **182,** 389 (1997).